Soil Potassium Sensor Using a Valinomycin-Decorated Reduced Graphene Oxide (rGO-v)-Based Field-Effect Transistor for Precision Farming

Nimisha, None; Sett, Avik; Tewari, Virendra Kumar; Bhattacharyya, Tarun Kanti

DOI
10.1021/acsagscitech.4c00406

Publication date
2024

Document Version
Final published version

Published in
ACS Agricultural Science and Technology

Citation (APA)
Nimisha, N., Sett, A., Tewari, V. K., & Bhattacharyya, T. K. (2024). Soil Potassium Sensor Using a Valinomycin-Decorated Reduced Graphene Oxide (rGO-v)-Based Field-Effect Transistor for Precision Farming. *ACS Agricultural Science and Technology*, *4*(10), 1112-1119. https://doi.org/10.1021/acsagscitech.4c00406

ACS AGRICULTURAL SCIENCE & TECHNOLOGY

pubs.acs.org/acsagscitech Article

Soil Potassium Sensor Using a Valinomycin-Decorated Reduced Graphene Oxide (rGO-v)-Based Field-Effect Transistor for Precision Farming

Published as part of ACS Agricultural Science & Technology special issue "Emerging Nano-Enabled Technologies for Sustainable Food and Agriculture".

Nimisha, Avik Sett, Virendra Kumar Tewari, and Tarun Kanti Bhattacharyya*

Cite This: ACS Agric. Sci. Technol. 2024, 4, 1112−1119 Read Online

ACCESS | Metrics & More | Article Recommendations | Supporting Information

ABSTRACT: A precise measurement of soil potassium (K) concentration is crucial for enhancing agricultural productivity and promoting sustainable land management. The efficiency of real-time soil quality monitoring is hampered by the time-consuming laboratory analysis that is commonly associated with conventional methods. The present research introduces an innovative approach utilizing a field-effect transistor (FET) structure coated with reduced graphene oxide-decorated valinomycin (rGO-v) for the detection of potassium ions in soil samples. The sensor exploits the distinctive electrical properties of reduced graphene oxide (rGO) and the specific affinity of valinomycin for potassium ions. To construct the device, we applied rGO-v onto an FET substrate. The conductance of the FET can be modified by the interaction between valinomycin and potassium ions, enabling the detection of potassium ions. Some of the advantages of this technology are its high sensitivity, fast response time, and potential for miniaturization. In addition, the device is tuned to demonstrate an enhanced sensitivity of 0.98 μA/(kg/ha) below the threshold voltage. The sensor exhibits a response time of 40 s and demonstrates exceptional stability in the face of unfavorable conditions, specifically humidity. Therefore, valinomycin-decorated reduced graphene oxide, when subjected to appropriate gate bias, demonstrates promising results as a versatile, cost-effective, and easy-to-use potassium ion sensor.

KEYWORDS: *reduce graphene oxide (rGO), valinomycin, field-effect transistor (FET) sensor, selectivity, soil testing*

1. INTRODUCTION

Potassium is a vital nutrient for crop growth and is essential for evaluating soil fertility.[1] It promotes several metabolic processes in plants, augments the regulatory ability of plant cells in reaction to environmental fluctuations, and boosts resistance to pests and lodging.[2] Monitoring soil potassium levels is crucial for improving agricultural productivity, as variations can lead to reduced crop yields and compromised soil fertility.[3−11] Conventional techniques for quantifying potassium levels, such as flame photometry, the difference method, and atomic absorption spectroscopy, provide benefits for measurement accuracy.[12,13] However, they are hindered by disadvantages such as protracted procedures, complex experimental methodologies, and significant environmental contamination. Moreover, survey data may have a lag issue, which may not satisfy the dynamic monitoring requirements of soil quality.[14,15] Therefore, establishing a quick and accurate measurement of the potassium level is essential for evaluating and monitoring soil properties. Two-dimensional materials including graphene, MoS_2, and WS_2 have been used for fabrication of various sensors (gas sensor, heavy metal ion sensor, biomolecule sensor, etc.). However, there is a lack of study of two-dimensional nanomaterials in the field of soil sensors. Hence, to address these issues and research gap, functionalized reduced graphene oxide-based field-effect transistor (FET)[16−18] sensors are being contemplated for the purpose of real-time monitoring of soil nutrients due to their high sensitivity, rapid response, and compatibility with wireless sensor networks. These sensors offer the benefit of immediate and uninterrupted monitoring of soil conditions, allowing farmers to make prompt decisions about fertilizer application and irrigation. Soil is a mixture of various elements that can interfere with the measurement process. To prevent this, two strategies are employed in this research study. The first one is the channel material in FET-based soil potassium sensors that consists of valinomycin ($C_{54}H_{90}N_6O_{18}$) coated with reduced graphene oxide (rGO-v). Valinomycin plays a critical role in determining the sensor's ability to selectively and sensitively detect potassium ions.[19,20] Additionally, reduced graphene oxide (rGO) offers a high surface area-to-volume ratio and acts as an insulation layer at the Si/SiO_2 interface. Valinomycin facilitates the selective transportation of potassium ions across lipid bilayers or ion channels by forming stable complexes with

Received: July 16, 2024
Revised: October 2, 2024
Accepted: October 3, 2024
Published: October 9, 2024

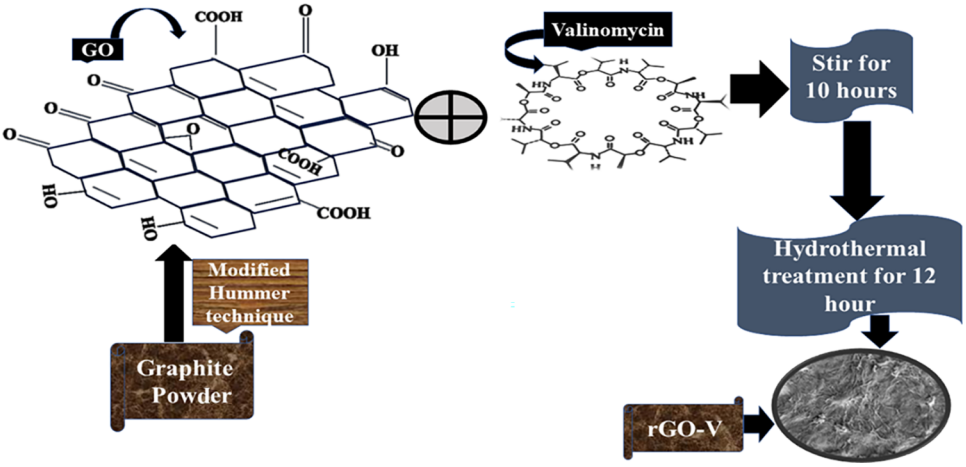

Figure 1. Synthesis procedure of the rGO-v sensing layer.

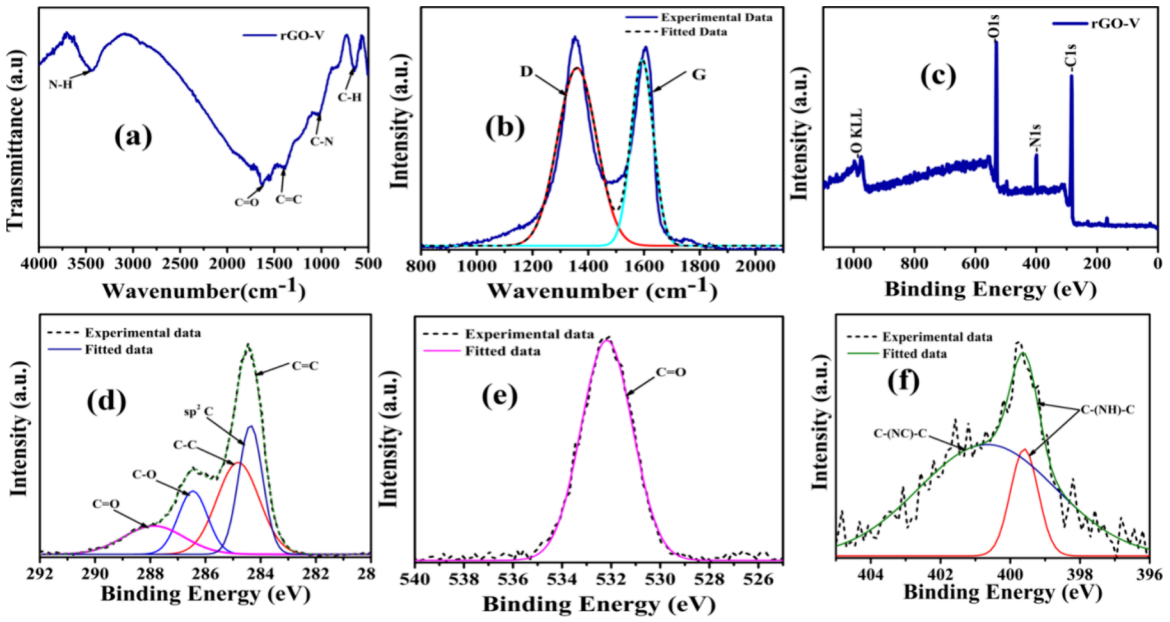

Figure 2. (a) FTIR spectra of rGO-v. (b) Raman spectra of rGO-v. (c) XPS survey scan of rGO-v. (d) High-resolution scan of carbon. (e) High-resolution scan of oxygen. (f) High-Resolution scan of nitrogen.

K^+ ions. The second method involves adjusting the gate potential to account for all potential interfering ions. Since each element has a unique ionization potential, it exhibits an optimal response at various gate voltages.

This research includes material synthesis, fabricating procedures, and characteristics of soil potassium sensors that use valinomycin-decorated reduced graphene oxide (rGO) as the channel material and are based on field-effect transistors (FETs). The initial selectivity test was conducted to assess the sensor's cross sensitivity. The results indicated that the sensor exhibited a 10% response to phosphorus, 20% response to nitrogen, and 99.6% response for the potassium ion. Consequently, the gate voltage was varied between −2 and 6 V to evaluate the sensor's response to nitrogen, phosphorus, and potassium ions. It was observed that the sensor demonstrated the highest response to nitrogen at 1.5 V (20%), while the response to phosphorus was around 2 V (10%), and for potassium, it was at 1 V (99.6%) gate potential. Therefore, the cross sensitivity is reduced to a large extent. This study has been performed by considering the potential applications of the sensors in precision agriculture, soil management, and environmental monitoring, with a focus on their significance in promoting sustainable crop production and soil health management

2. EXPERIMENTAL SECTION

2.1. Synthesis of rGO-v. The synthesis of graphene oxide (GO) was achieved by chemically exfoliating graphite powder by using a modified Hummer process, as shown in Figure 1. A precise amount of 3.4 g of powdered graphite, obtained from Sigma-Aldrich, was combined with 1.8 g of sodium nitrate ($NaNO_3$), acquired from MERCK. The resulting combination was stirred for a duration of 48 h in 69 mL of 98% sulfuric acid (H_2SO_4), also obtained from MERCK. Following 10 h of stirring, the solution was transferred to an ice bath at a temperature of 0 °C for a duration of 15 min.[21] Afterward, a total of 9.7 g of potassium permanganate was slowly added to the solution while making sure that the temperature stayed below 10 °C. The solution was placed on a hot plate set to 35 °C to reach an equilibrium temperature the same as room temperature. After the mixture reached room temperature, 150 mL of deionized (DI) water was added to initiate the exothermic oxidation reaction, resulting in

https://doi.org/10.1021/acsagscitech.4c00406
ACS Agric. Sci. Technol. 2024, 4, 1112−1119

increasing of temperature to 98 °C. After a 20 min exothermic reaction, the process is suddenly stopped by submerging the container in a water bath at a temperature of 35 °C. The solution underwent a color transformation, transitioning from a brown to a black hue. After a duration of 40 min, a volume of 500 mL of deionized (DI) water and 12 mL of hydrogen peroxide with a concentration of 30% was added to the brown solution. The solution undergoes a transformation and turns into a vivid yellow GO. The yellow solution was subjected to centrifugation, and the resulting solid particles were collected after being rinsed with 37% hydrochloric acid. The pH of the solution was regularly kept at a neutral level of seven by continuously washing it with deionized water (DI). After the desired pH level was achieved, the layer of pure GO slurry was moved to a separate container. Next, 5 mL of produced graphene oxide (GO) was mixed with 100 mL of deionized (DI) water and continuously stirred for 1 h at a speed of 800 rpm (rpm). Subsequently, a volume of 0.5 mL of valinomycin solution already dissolved in DMSO (obtained from Sigma-Aldrich) was added to it. Then, the whole solution was stirred for 4 h at a temperature of 5 °C so that GO is functionalized with the valinomycin layer. Once GO was functionalized, then the whole solution was put into a Teflon-lined hydrothermal autoclave for hydrothermal treatment at 200 °C for 12 h. The resulting solution-based sensing layer was named rGO-v.

2.2. Material Characterization. Figure 2a shows the FTIR analysis of rGO-v, which is a technique employed to examine the functional groups in the sensing layer by analyzing its vibrational frequency. The spectrum has peaks at 3428.72, 1629.08, 1391.82, 1015.74, and 638.82 cm^{-1}, which correspond to the presence of NH, C=O, C=C, C−N, and C−H, respectively. Valinomycin is composed of alternating amide and ester groups, which can be confirmed by the presence of NH and C=O groups through FTIR analysis.[22] C=C, C−H is present due to the aromatic carbon ring. Valinomycin's ability to readily bind metal ions is facilitated by the presence of the carbonyl group and its distinctive doughnut-shaped structure.

Figure 2b shows the Raman spectroscopy of rGO-v having the I_D/I_G of approximately 1.045, which shows a huge number of defects present at the surface.[23] Figure 2c depicts the XPS survey scan of rGO-v. The survey scan analysis indicates the presence of carbon, oxygen, and nitrogen at energy levels of 283.9, 533.34, and 400.86 eV, respectively. The high-resolution (HR) scan of carbon indicates the presence of several chemical bonds. Peaks at 284.4, 284.3, 284.8, 286.46, and 287.92 eV correspond to the presence of C=C, sp^2C, C−C, C−O, and C=O bonds,[24] respectively, as depicted in Figure 2d. The HR scan of oxygen has a prominent peak at 532.15 eV, which corresponds to the C=O bond depicted in Figure 2e. The high-resolution scan of nitrogen reveals a peak at 399.58 and 400 eV for the C−(NH)−C and C−(NC)−C bonds,[25] respectively, as depicted in Figure 2f. Figure 3 shows the FESEM image of rGO-v from low to high magnification. The sheet-like structure of the sensing layer ensures high specific surface area, which is highly beneficial for sensing efficiency.

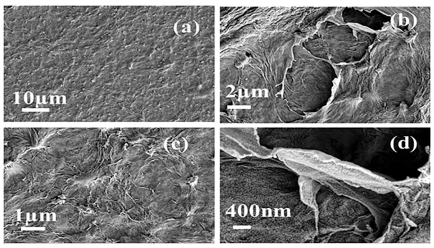

Figure 3. FESEM analysis of rGO-v.

2.3. Fabricated Device Structure and Experimental Setup. A p+⟨100⟩ silicon wafer, which has been doped with boron and has a resistivity of 0.001 ohm-cm, was utilized as the substrate for the fabrication of the device. A 120 nm layer of SiO_2 was grown by thermal oxidation using a dry (10 min)−wet (5 min)−dry (10 min) technique. The shadow mask was necessary to create the back gate. The degenerately doped silicon wafer was used as the back gate. The edge of the SiO_2 coated wafer was masked with Kapton tape and spin-coated with positive photoresist at 3000 rpm for 30 s. The wafer was then baked for 30 min, the Kapton tape was removed, and the etching of the Si/SiO_2 wafer (20 min) was performed using BHF to create the back gate. Then, for further source and drain patterns, an interlayer of titanium (Ti) with a thickness of 15 nm was employed to enhance the adhesion of Au (Au) on SiO_2. On top of the titanium (Ti) layer, 180 nm thick gold was deposited using DC sputtering. The gold (Au) and titanium (Ti) layers underwent a lithographic procedure to create source and drain electrodes, which had a width of 240 μm and a channel gap of 30 μm. For photolithography, positive photoresist of AZ series was used, and it coated the wafer at 500 rpm for 5 s and then 3000 rpm for 20 s. After that, it was prebaked for 5 min at 90 °C, and then the mask and wafer (resist coated) were loaded to the double-sided mask aligner, and it was exposed to UV rays for 10 s. Then, it was developed and postbaked at 120 °C for 5 min. Further gold and titanium etchant was used to etch the device. In the last, a stripper was used to strip the photoresist. Finally, the device was ready for channel formation. Figure 4a depicts a schematic of the fabricated device and experimental setup. PLV-50 was used for probing the device, and the B1500A semiconductor parameter analyzer was used for the analysis of the data. Figure 4b depicts the camera image of the probe station probed with the fabricated device structure. Priorly synthesized rGO-v was precisely placed by drop casting it between the source and drain electrodes using a specialized drop casting instrument known as a Nano enabler.

3. RESULT AND DISCUSSION

3.1. Device Characterization. The transfer characteristics of the FET rGO-v were plotted by varying the gate-to-source voltage (−10 to +10 V) and capturing the drain current at the fixed drain-to-source voltage (1−4 V), as shown in Figure 5a. Transfer characteristics are ambipolar in nature, which clearly indicates the presence of electrons and holes.[26] When the gate-to-source voltage (V_{gs}) is negative, then the Fermi level at the gate end moves upward, and a small positive drain-to-source voltage (V_{ds}) leads to a slight bending of the Fermi level down at the drain end.[27] Thus, holes will start flowing from the drain to the source, and as the current flows in the direction of the hole, current I_{ds} is captured. When the positive gate voltage is applied, it pulls down the Fermi level, and electrons will start moving from the source to the drain. Then, the electron current will flow from the drain to the source, but in this material, as holes are predominant, the hole current is observed to exceed electron current. The threshold voltage of the device is +1.9 V. Output characteristics of the device are plotted between drain-to-source voltage (V_{ds}) and drain-to-source current (I_{ds}) at different gate-to-source voltages (V_{gs}). In this work, V_{ds} is varied from 0 to 5 V and I_{ds} is captured at different V_{gs} (1−5 V) as shown in Figure 5b. The device shows ohmic characteristics as $\varnothing_{Au} > \varnothing_{rGO\text{-}v}$. Output current I_{ds} is observed to increase as V_{gs} increases in the positive direction.[28−30]

3.2. Selectivity Analysis. A selectivity test of the sensing layer is carried out at 4 ppm concentration for all possible ions, namely, nitrogen(N), phosphorus(P), potassium(K), calcium (Ca), magnesium (Mg), sulfur (S), zinc (Zn), copper (Cu), iron (Fe), boron (Br), chlorine (Cl), and nickel (Ni). It is found that the sensor device demonstrated a significant response for NPK, i.e., 20,10, and 99.6%, respectively. The device showed negligible response toward other elements shown in Figure 6a. Hence, a gate effect study is carried out for nitrogen, phosphorus, and potassium, as shown in Figure 6b,c,d, respectively. Initially all of the tests were carried out

https://doi.org/10.1021/acsagscitech.4c00406
ACS Agric. Sci. Technol. 2024, 4, 1112−1119

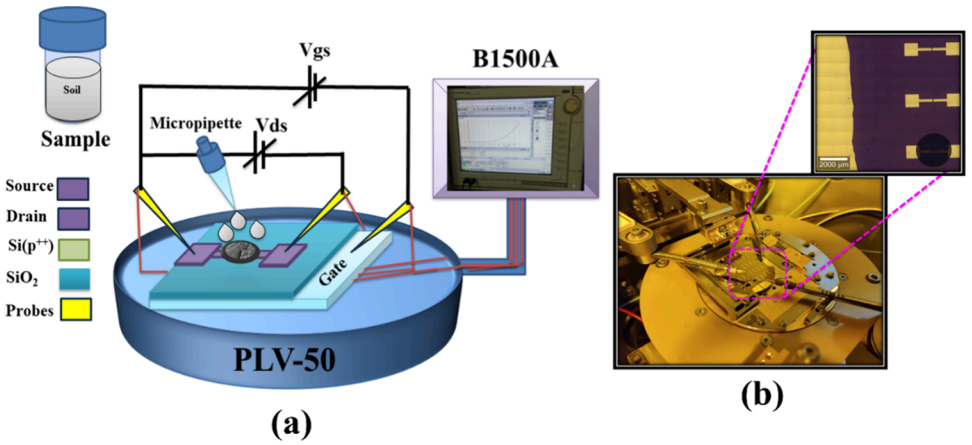

Figure 4. (a) Schematic of the device with the complete experimental setup. (b) Fabricated device.

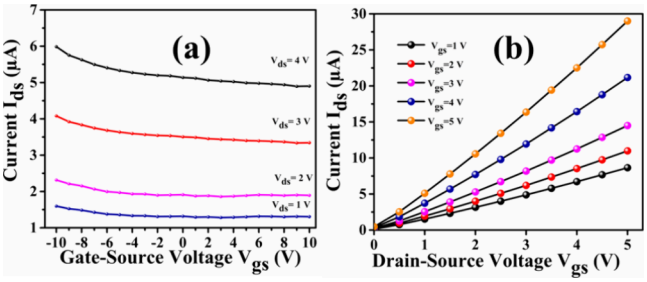

Figure 5. (a) Transfer characteristics of the rGO-v FET device. (b) Output characteristics of the rGO-v FET device.

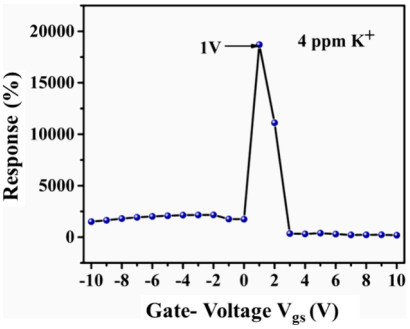

Figure 7. Response of the sensor due to the potassium ion.

with standard salt solutions. Later on, the device is tested on soil samples.

3.3. Response of the Sensor. Figure 7 depicts the variation of the sensor response at 4 ppm potassium ion concentration at different gate-to-source voltages (V_{gs}). The highest response of the device is obtained at V_{gs}= 1 V. The threshold voltage of the device is 1.9 V, below which carrier concentration in the channel is negligible and imparts very high sensing response, due to a higher charge transfer ratio.

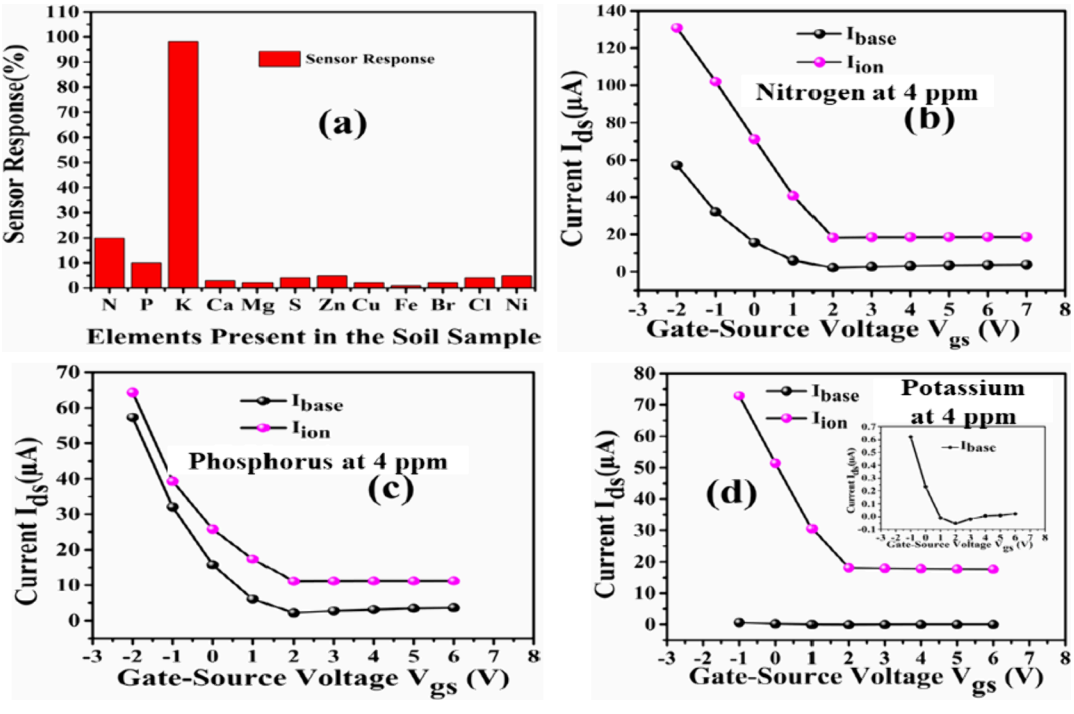

Figure 6. (a) Selectivity analysis. (b) Gate effect on the ammonium ion. (c) Gate effect on the phosphate ion. (d) Gate effect on the potassium ion.

https://doi.org/10.1021/acsagscitech.4c00406
ACS Agric. Sci. Technol. 2024, 4, 1112−1119

The sensing response is given by a number of positive charges donated by the potassium ion to the original number of holes in the channel. At V_{gs} = 1 V, the number of holes in the channel is such that the K^+ ion is detected with the highest sensitivity. With the increase in the gate voltage (V_{gs}), the number of free holes increases in the channel and the fraction of holes lost decreases. That is why response gets reduced. Therefore, the optimized gate voltage for the highest response is 1 V.

3.4. Testing of the Device with the Soil Sample. The preparation of soil samples involves combining 1.5 g of desiccated soil with 60 mL of deionized water. Subsequently, it underwent ultrasonication for a duration of 20 min and was utilized for the initial test results. After that, 20 mL of soil sample was extracted, and an equal volume of deionized water (DI water) was introduced to obtain the second density. Table 1 provides a concise summary of the test outcomes. The sensor's output is directly proportional to the concentration of potassium in the soil. However, the accuracy of detection decreases as more deionized water is added to the sample.

Table 1. Sensor Response Measurement for Available Potassium in the Listed Soil Sample

S.no	soil sample name	potassium (kg/ha)	sensor response (%)
1	Jintur-1	739.3	9900
2	Jintur-2	719.72	3471.42
3	Manwat-1	591.13	733.33
4	Italapur-1	590.1	669.23
5	Ujawala-Phata	476.45	369.48
6	Manwat-2	365.68	334.68

Figure 8 depicts the output characteristic (I_{ds}−V_{ds}) of the device at the optimum gate voltage (1 V) for six distinct black soil samples with varying soil potassium (K^+) contents. It was noticed that when the concentration of potassium(K^+) ions in the soil increases, the current passing through the device also increases. This is due to a large number of positive charges being transported from potassium (K^+) to the rGO-v sensing layer, resulting in an increase in the hole concentration.

Figure 9 depicts the sensitivity of the device toward the potassium ion (K^+) at 1 V gate-to-source bias voltage. The sensitivity of the device is calculated at various potassium concentrations in soil, i.e., 365.68, 476.45, 590.1, 591.13, 719.72, and739.3 kg/ha. It is found that the sensitivity of the device is 0.98 μA/(kg/ha) at a gate voltage of 1 V, and device sensitivity increases as the potassium ion increases in the soil sample.

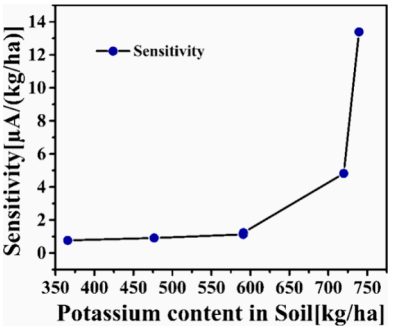

Figure 9. Sensitivity of the device due to the potassium ion present in the soil sample.

Figure 10a depicts the sensor response at different density levels at different potassium ion concentrations. It is clearly observed that as density keeps on reducing, it is very difficult to predict the actual potassium ion present in the soil sample. Therefore, the optimized soil density is 1.5−2.5 g for the soil sample. In this research work, 1.5 g of soil sample is used for all kinds of analysis purposes.

The valinomycin-decorated reduced graphene oxide (rGO-v) is the composite material that enhances stability and reduces interaction with water molecules, resulting in decreased sensitivity to humidity. Valinomycin is a natural ionophore that is hydrophobic in nature. When it is attached to the surface of rGO, it creates a hydrophobic layer on rGO that repels the water molecules and makes it insensitive to humidity, as shown in Figure 10b. Figure 10c depicts the transient analysis of rGO-v at three different concentrations of

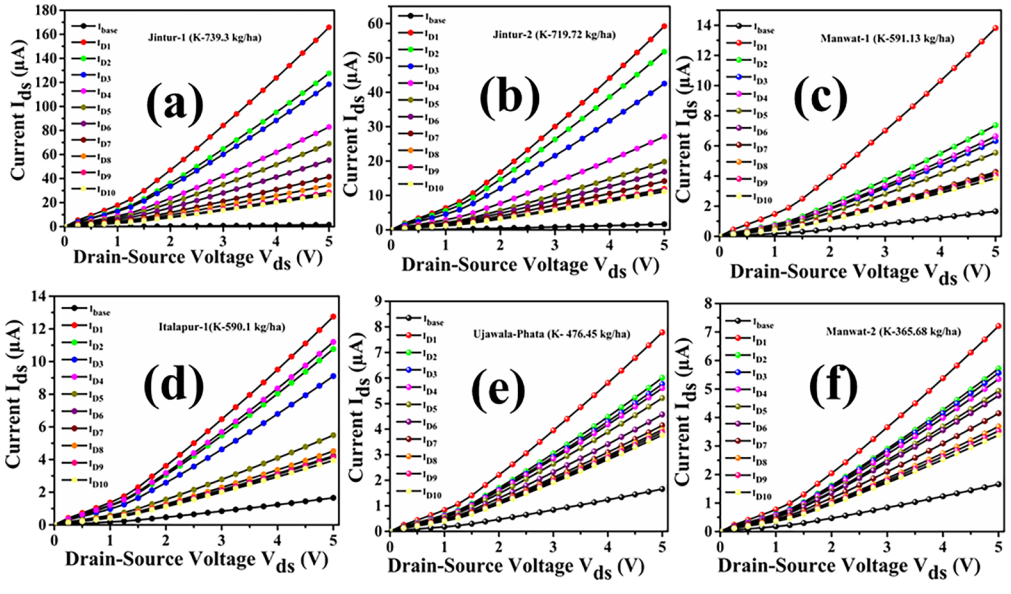

Figure 8. Six different soil samples with linear density variation.

https://doi.org/10.1021/acsagscitech.4c00406
ACS Agric. Sci. Technol. 2024, 4, 1112−1119

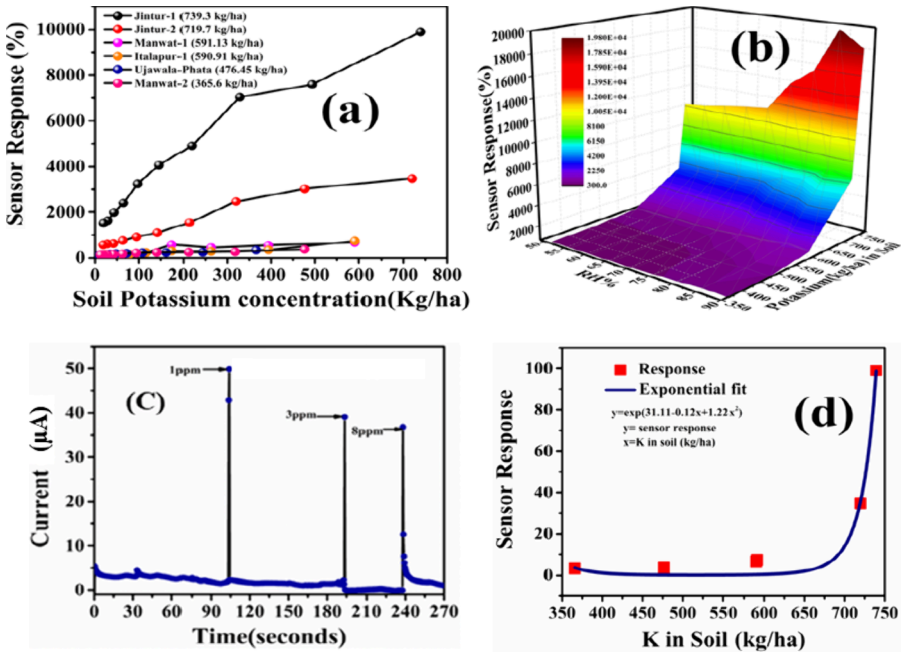

Figure 10. (a) Sensor response for different soil potassium concentrations. (b) Response vs humidity plot. (c) Transient analysis of the device. (d) Calibration scale for the potassium ion in the soil sample.

1, 3, and 8 ppm. Transient analysis involves studying the behavior of the material over time when the sensor is exposed to three different potassium ion concentrations. Initially, when the sensor is unexposed to ions, all active sites are free to interact, and when 1 ppm of potassium ion solution is drop-casted, it shows a 45 μA variation in the current. Subsequently, when 3 and 8 ppm potassium ion solution is drop-casted, then the change in current reduced to 35 and 30 μA because of the already occupied active sites. Figure 10d depicts the final calibration curve of the sensor. It depicts the sensor response at different potassium ion concentrations. The equation is given as

$$y = \exp(31.11 - 0.12x + 1.22x^2) \quad (1)$$

where y is the sensor response and x is the potassium(kg/ha) ion in the soil sample.

Three batches of the sensor material was synthesized, and subsequently, the devices were fabricated. Three sets of devices were fabricated out of three batches and were tested for reproducibility of the method toward NPK response. All of the devices were tested at 4 ppm concentration. The experiments verify high reproducibility of the sensors and the fabrication methods as shown in Table 2.

3.5. Sensing Mechanism. Valinomycin is a macrocyclic molecule composed of 12 alternating amino acid and ester units, with a chemical formula of $C_{54}H_{90}N_{60}O_{18}$. The presence of these 12 carbonyl groups is crucial for their ability to pair with metal ions. It comprises oxygen-containing functional groups that are readily capable of accepting electrons. When the valinomycin molecule binds to the rGO surface, a bond is established between the carboxylic group (COOH) and the amine group of the valinomycin. The process involves the creation of a single electron-accepting site within the material, causing a change in the Fermi level of the valinomycin-decorated reduced graphene oxide (rGO) toward the valence band. Thus, the material exhibits p-type conductivity, indicating the dominance of holes.

When a soil sample is drop-cast over it, potassium ions become trapped within the immediate vicinity of the valinomycin, as depicted in Figure 11.

$$\text{rGO} - \text{COOH} + \text{valinomycin} - \text{NH}_2 \rightarrow \text{rGO} - v + \text{by products} \quad (2)$$

Comparison with some existing technology (Table 3) proves that the proposed device and method can be fast, efficient, and highly accurate.

In this research work, the utilization of valinomycin-decorated reduced graphene oxide (rGO-v) offers a highly opportune method for creating a potassium ion sensor that can be used in soil sensing applications. Tuning the gate voltage of the device reduces the interference coming from other elements present in the soil sample. This sensor offers a superior level of sensitivity, selectivity, and stability. This technological innovation has significant potential to enhance agricultural operations and maximize crop yields by accurately detecting the potassium levels in soil samples. However, the current research limits the reusability of the sensor device and exposure to dynamic environmental parameters. Research in the direction of reusability and proper packaging of the device would improve the cost effectiveness, stability, and performance of the proposed sensor device. Moreover, the

Table 2. Reproducibility of the Fabricated Devices toward NPK

devices	response to nitrogen	response to phosphorus	response to potassium
device from batch 1	20%	10%	99.6%
device from batch 2	19.3%	10.7%	99.2%
device from batch 3	18.9%	9.6%	99.4%

https://doi.org/10.1021/acsagscitech.4c00406
ACS Agric. Sci. Technol. 2024, 4, 1112−1119

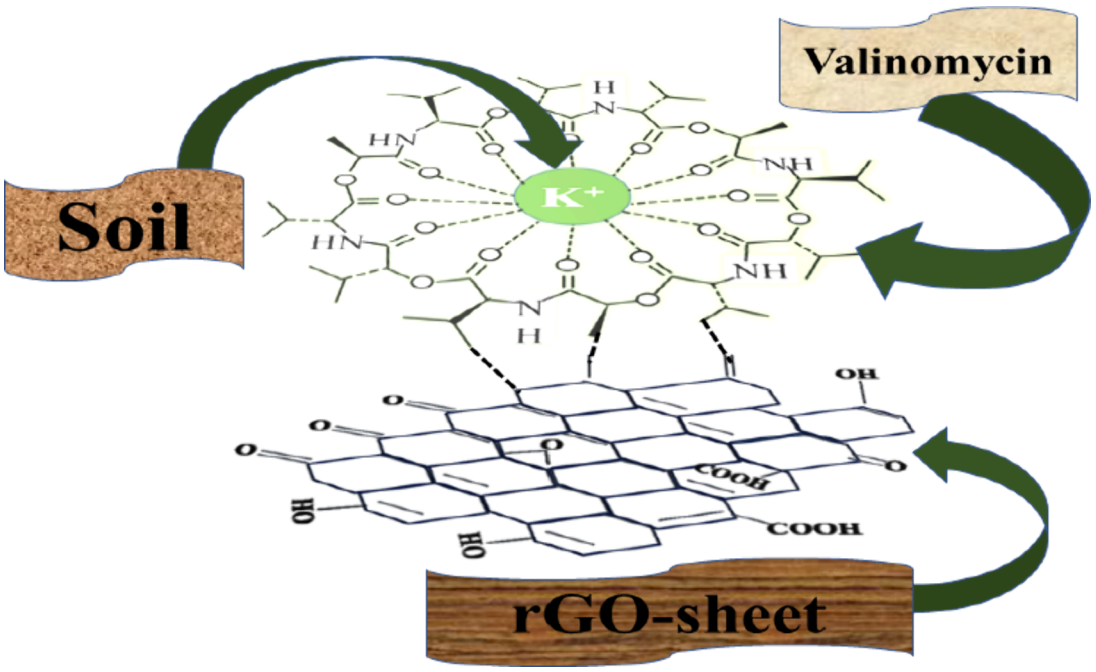

Figure 11. Sensing Mechanism of the K+ ion in the soil sample.

Table 3. Comparison with Existing Methods

detection method	process time	LOD	sensitivity	reference
atomic absorption spectrometry	1−2 h	0.1 ppm	1 ppb	31
inductively coupled plasma spectrometry	∼1 h	0.005−0.0025 mg/kg		32
flame photometry	1 min	0.1−1 mg/L		33
rGO-v FET	∼50 s	1 ppb	0.98 μA/kg/ha	this work

combination of sensor arrays with machine learning algorithms would ensure tremendous selectivity toward determining the NPK content of the soil. This research work provides the basis for the development of sensor arrays. Each sensor in the array, if optimized to a sensitive gate potential as discussed in this work, would provide accurate NPK levels during soil quality monitoring.

■ ASSOCIATED CONTENT

Supporting Information

The Supporting Information is available free of charge at https://pubs.acs.org/doi/10.1021/acsagscitech.4c00406.

EDX analysis of GO and rGO-v (Figures S1 and S2) (PDF)

■ AUTHOR INFORMATION

Corresponding Author

Tarun Kanti Bhattacharyya − *Electronics and Electrical Communication Engineering, IIT Kharagpur, Kharagpur, West Bengal 721302, India;* orcid.org/0000-0002-7699-6436; Email: tkb@ece.iitkgp.ac.in

Authors

Nimisha − *Electronics and Electrical Communication Engineering, IIT Kharagpur, Kharagpur, West Bengal 721302, India*

Avik Sett − *Department of Microelectronics, Delft University of Technology, Delft, CD 2628, Netherlands;* orcid.org/0000-0001-8437-607X

Virendra Kumar Tewari − *Agricultural and Food Engineering, IIT Kharagpur, Kharagpur, West Bengal 721302, India*

Complete contact information is available at: https://pubs.acs.org/10.1021/acsagscitech.4c00406

Author Contributions

Nimisha: investigation, methodology, writing—original draft, data curation, formal analysis. Avik Sett: validation, writing—review and editing. Virendra Kumar Tewari: supervision, validation, funding acquisition Tarun Kanti Bhattacharyya: conceptualization, validation, writing—review and editing, supervision, funding acquisition, project administration.

Funding

Meity and DST, Govt. of India.

Notes

The authors declare no competing financial interest.

■ ACKNOWLEDGMENTS

The authors wish to acknowledge the project sponsored by Meity and DST, Govt. of India, for funding support during the work.

■ ABBREVIATIONS

GO-graphene oxide; rGO-reduce graphene oxide; FET-field-effect transistor; FTIR-Fourier-transform infrared spectroscopy; SEM-scanning electron microscopy; XPS-X-ray photoelectron spectroscopy

REFERENCES

(1) Munnaf, M. A.; Guerrero, A.; Nawar, S.; Haesaert, G.; Van Meirvenne, M.; Mouazen, A. M. A combined data mining approach for on-line prediction of key soil quality indicators by Vis-NIR spectroscopy. *Soil Tillage Res.* **2021**, *205*, No. 104808.

(2) Mozaffari, H.; Moosavi, A. A.; Ostovari, Y.; Nematollahi, M. A.; Rezaei, M. Developing spectrotransfer functions (STFs) to predict basic physical and chemical properties of calcareous soils. *Geoderma* **2022**, *428*, No. 116174.

(3) Brady, N. C.; Weil, R. R. *The nature and properties of soils*; Prentice Hall: Upper Saddle River, NJ, (2008) Vol. *13*.

(4) Mohammad, M. J.; Mazahreh, N. Communications in soil science and plant analysis changes in soil fertility parameters in response to irrigation of forage crops with secondary treated wastewater. *Commun. Soil Sci. Plant Anal.* **2003**, *34*, 1281−1294.

(5) Tadesse, T.; Dechassa, N.; Bayu, W.; Gebeyehu, S. Effects of farmyard manure and inorganic fertilizer application on soil physicochemical properties and nutrient balance in rain-fed lowland rice ecosystem. *Am. J. Plant Sci.* **2013**, *4* (2), 28313.

(6) Agbeshie, A. A.; Abugre, S.; Adjei, R.; Atta-Darkwa, T.; Anokye, J. Impact of land use types and seasonal variations on soil physicochemical properties and microbial biomass dynamics in a tropical climate, Ghana. *Adv. Res.* **2020**, *21* (1), 34−49.

(7) Burton, L.; Jayachandran, K.; Bhansali, S. Review—The 'realtime' revolution for in situ soil nutrient sensing. *J. Electrochem. Soc.* **2020**, *167* (3), No. 037569.

(8) Jahany, M.; Rezapour, S. Assessment of the quality indices of soils irrigated with treated wastewater in a calcareous semi-arid environment. *Ecological Indicators* **2020**, *109*, No. 105800.

(9) Lal, R. Managing soils for negative feedback to climate change and positive impact on food and nutritional security. *Soil Sci. Plant Nutrition* **2020**, *66* (1), 1−9.

(10) Grusak, M. A.; Broadley, M. R.; White, P. J. *Plant Macro- and Micronutrient Minerals*; Wiley: Hobo-ken, NJ, USA, 2016. .

(11) Fontana, J. E.; et al. Impact of potassium deficiency on cotton growth, development and potential mi-croRNA-mediated mechanism. *Plant Physiol. Biochemistry* **2020**, *153*, 72−80.

(12) Ruangratanakorn, J.; Suwonsichon, T.; Kasemsumran, S.; Thanapase, W. Installation design of on-line near infrared spectroscopy for the production of compound fertilizer. *Vib. Spectrosc.* **2020**, *106*, No. 103008.

(13) Du, X.; Chen, H.; Xie, J.; Li, L.; Cai, K.; Meng, F. Quantitative analysis of soil potassium by near-infrared (NIR) spectroscopy combined with a three-step progressive hybrid variable selection strategy. *Spectrochim Acta A Mol. Biomol Spectrosc* **2025**, *324*, No. 124998.

(14) Das, D.; Dwivedi, B. S.; Datta, S. P.; Datta, S. C.; Meena, M. C.; Agarwal, B. K.; Shahi, D. K.; Singh, M.; Chakraborty, D.; Jaggi, S. Potassium supplying capacity of a red soil from eastern India after forty-two years of continuous cropping and fertilization. *Geoderma* **2019**, *341*, 76−92.

(15) Islam, S.; Timsina, J.; Salim, M.; Majumdar, K.; Gathala, M. Potassium supplying capacity of diverse soils and K-use efficiency of maize in South Asia. *Agronomy- Basel* **2018**, *8*, 121.

(16) Cai, B.; Xia, Z.; Wang, J.; Wu, S.; Jin, X. Reduced Graphene Oxide-Based Field Effect Transistor Biosensors for High-Sensitivity miRNA21 Detection. *ACS Appl. Nano Mater.* **2022**, *5* (8), 12035−12044.

(17) Aspermair, P.; Mishyn, V.; Bintinger, J.; Happy, H.; Bagga, K.; Subramanian, P.; Knoll, W.; Boukherroub, R.; Szunerits, S. Reduced graphene oxide-based field effect transistors for the detection of E7 protein of human papillomavirus in saliva. *Anal. Bioanal. Chem.* **2021**, *413* (3), 779−787.

(18) Sengupta, J.; Hussain, C. M. Graphene-based field-effect transistor biosensors for the rapid detection and analysis of viruses: A perspective in view of COVID-19. *Carbon Trends* **2021**, *2*, No. 100011.

(19) Tharini, C.; Iyappan, G.; Manikandan, E.; Sephra, P. J. Potentiometric sensing of potassium ion (K+) using valinomycin supported on ZnO/rGO nanocomposites. *Journal of Materials Science: Materials in Electronics* **2023**, *34* (19), 1474.

(20) Zainudin, A. A.; Fen, Y. W.; Yusof, N. A.; Al-Rekabi, S. H.; Mahdi, M. A.; Omar, N. A. S. Incorporation of surface plasmon resonance with novel valinomycin doped chitosan-graphene oxide thin film for sensing potassium ion. *Spectrochim. Acta, Part A* **2017**, *191*, 111−115.

(21) Sett, A.; Bhattacharyya, T. K. Functionalized gold nanoparticles decorated reduced graphene oxide sheets for efficient detection of mercury. *IEEE Sensors J.* **2020**, *20* (11), 5712−5719.

(22) Fonina, L. A.; Sanasaryan, A. A.; Vinogradova, E. I. Synthesis of analogs of valinomycin with modified side chains and different contents of amide and ester groups. *Chem. Nat. Compd.* **1971**, *7* (1), 62−71.

(23) Yamamoto, S.; Straka, M.; Watarai, H.; Bouř, P. Formation and structure of the potassium complex of valinomycin in solution studied by Raman optical activity spectroscopy. *Phys. Chem. Chem. Phys.* **2010**, *12* (36), 11021−11032.

(24) Chen, X.; Wang, X.; Fang, D. A review on C1s XPS-spectra for some kinds of carbon materials. *Fullerenes, Nanotubes Carbon Nanostruct.* **2020**, *28* (12), 1048−1058.

(25) Yamada, Y.; Kim, J.; Matsuo, S.; Sato, S. Nitrogen-containing graphene analyzed by X-ray photoelectron spectroscopy. *Carbon* **2014**, *70*, 59−74.

(26) Jmai, B.; Silva, V.; Mendes, P. M. 2D electronics based on graphene field effect transistors: Tutorial for modelling and simulation. *Micromachines* **2021**, *12* (8), 979.

(27) Chaves, F. A.; Jimenez, D. The role of the Fermi level pinning in gate tunable graphene-semiconductor junctions. *IEEE Trans. Electron Devices* **2016**, *63* (11), 4521−4526.

(28) Sett, A.; Sarkar, L.; Majumder, S.; Bhattacharyya, T. K. Amplification of ammonia sensing performance through gate induced carrier modulation in Cur-rGO Silk-FET. *Sci. Rep.* **2023**, *13* (1), 8159.

(29) Chen, Y.; et al. Field-Effect Transistor Biosensor for Rapid Detection of Ebola Antigen. *Sci. Rep* **2017**, *7* (1), 10974.

(30) Nimisha; Sett, A.; Tewari, V. K.; Bhattacharyya, T. K. Tuning of gate electrostatics to amplify mercury sensing performance of functionalized field effect transistor. *IEEE Sens. J.* **2024**, 1.

(31) David, D. J. The determination of exchangeable sodium, potassium, calcium and magnesium in soils by atomic-absorption spectrophotometry. *Analyst* **1960**, *85* (1012), 495−503.

(32) Nageswaran, G.; Choudhary, Y. S.; Jagannathan, S. Chapter 8 - Inductively Coupled Plasma Mass Spectrometry. In *Spectroscopic Methods for Nanomaterials Characterization*, Thomas, S.; Thomas, R.; Zachariah, A. K.; Mishra, R. K., Eds., Elsevier: 2017; pp 163−194. doi: .

(33) Brealey, L. The determination of potassium in fertilisers by flame photometry. *Analyst* **1951**, *76* (903), 340−343.

https://doi.org/10.1021/acsagscitech.4c00406
ACS Agric. Sci. Technol. 2024, 4, 1112−1119